

# **HIGH-RESOLUTION SEISMIC VELOCITY AND ATTENUATION MODELS OF EASTERN TIBET AND ADJACENT REGIONS (POSTPRINT)**

## **Annual Report 2**

**Xueyang Bao, et al.**

**University of Missouri  
316 University Hall  
Columbia, MO 65211-3020**

**4 June 2012**

**Technical Paper**

**APPROVED FOR PUBLIC RELEASE; DISTRIBUTION IS UNLIMITED.**



**AIR FORCE RESEARCH LABORATORY  
Space Vehicles Directorate  
3550 Aberdeen Ave SE  
AIR FORCE MATERIEL COMMAND  
KIRTLAND AIR FORCE BASE, NM 87117-5776**

REPORT DOCUMENTATION PAGE				Form Approved OMB No. 0704-0188	
Public reporting burden for this collection of information is estimated to average 1 hour per response, including the time for reviewing instructions, searching existing data sources, gathering and maintaining the data needed, and completing and reviewing this collection of information. Send comments regarding this burden estimate or any other aspect of this collection of information, including suggestions for reducing this burden to Department of Defense, Washington Headquarters Services, Directorate for Information Operations and Reports (0704-0188), 1215 Jefferson Davis Highway, Suite 1204, Arlington, VA 22202-4302. Respondents should be aware that notwithstanding any other provision of law, no person shall be subject to any penalty for failing to comply with a collection of information if it does not display a currently valid OMB control number. <b>PLEASE DO NOT RETURN YOUR FORM TO THE ABOVE ADDRESS.</b>					
1. REPORT DATE (DD-MM-YYYY) 04-06-2012		2. REPORT TYPE Technical Paper		3. DATES COVERED (From - To) 01 Sep 2010 to 19 Mar 2012	
4. TITLE AND SUBTITLE High-Resolution Seismic Velocity and Attenuation Models of Eastern Tibet and Adjacent Regions (Postprint) Annual Report 2				5a. CONTRACT NUMBER FA9453-10-C-0256	
				5b. GRANT NUMBER	
				5c. PROGRAM ELEMENT NUMBER 62601F	
6. AUTHOR(S) Xueyang Bao <sup>1</sup> , Eric A. Sandvol <sup>1</sup> , James Ni <sup>2</sup> , Tom Hearn <sup>2</sup> , Savas Ceylan <sup>1</sup> , Xiaofeng Liang <sup>1</sup> , and W. Scott Phillips <sup>3</sup>				5d. PROJECT NUMBER 1010	
				5e. TASK NUMBER PPM00005454	
				5f. WORK UNIT NUMBER EF004195	
7. PERFORMING ORGANIZATION NAME(S) AND ADDRESS(ES)  University of Missouri 316 University Hall Columbia, MO 65211-3020				8. PERFORMING ORGANIZATION REPORT NUMBER	
9. SPONSORING / MONITORING AGENCY NAME(S) AND ADDRESS(ES) Air Force Research Laboratory Space Vehicles Directorate 3550 Aberdeen Ave SE Kirtland AFB, NM 87117-5776				10. SPONSOR/MONITOR'S ACRONYM(S) AFRL/RVBYE	
				11. SPONSOR/MONITOR'S REPORT NUMBER(S) AFRL-RV-PS-TP-2012-0040	
12. DISTRIBUTION / AVAILABILITY STATEMENT Approved for public release; distribution is unlimited. (LA-UR-11-04823).					
13. SUPPLEMENTARY NOTES Published in The Proceedings of the 2011 Monitoring Research Review – Ground-Based Nuclear Explosion Monitoring Technologies, 13 – 15 September 2011, Tucson, AZ, Volume I, pp 21-29. Government Purpose Rights.  University of Missouri <sup>1</sup> , New Mexico State University <sup>2</sup> , and Los Alamos National Laboratory <sup>3</sup>					
14. ABSTRACT  High-resolution seismic velocity and attenuation models of the Tibetan Plateau and adjacent regions are critical to monitoring seismology efforts in Eurasia. Waveform data are collected from new deployed seismic networks including NETS (North-Eastern Tibet Seismic experiment), INDEPTH-IV-ASCENT, INDEPTH-IV-UK, and previous networks, comprising an unprecedented coverage of the eastern half of the Tibetan plateau. Three seismic methods are used in the velocity structure in this region: Pn velocity tomography, body-wave finite-frequency tomography, and Rayleigh wave phase velocity. Consistent anomalies in the crust and upper mantle are observed using all of these methods. These anomalies include a low velocity in northern Qiangtang and the Songpan-Ganzi fold belt and high velocity in the Qaidam Basin. QLg and QPg models have been determined using a Reverse Two-station/event Method, which shows a high seismic attenuation zone along the Kunlun belt. Significant azimuthal anisotropy of seismic Q also observed. The isotropic seismic Q, suggested as an estimate of QS for the crust, is low in northern Qiangtang and the Songpan-Ganzi. The high-Q directions parallel major fault planes in eastern Tibet, and correlate with fast-direction of shear wave splitting and Rayleigh wave azimuthal anisotropy fast directions, which suggests a coherency of deformation between the crust and upper mantle in this region. Similarly, a high velocity and high Q block in southeastern Tibet around eastern Bangong-Nujiang Suture and Eastern Himalaya Syntaxis correlates well with the high velocity in this region.					
15. SUBJECT TERMS Seismic velocity structure, Seismic attenuation structure, Eurasia					
16. SECURITY CLASSIFICATION OF:			17. LIMITATION OF ABSTRACT  Unlimited	18. NUMBER OF PAGES  12	19a. NAME OF RESPONSIBLE PERSON Robert J. Raistrick
a. REPORT Unclassified	b. ABSTRACT Unclassified	c. THIS PAGE Unclassified			19b. TELEPHONE NUMBER (include area code)

**HIGH-RESOLUTION SEISMIC VELOCITY AND ATTENUATION MODELS OF EASTERN TIBET  
AND ADJACENT REGIONS**

Xueyang Bao<sup>1</sup>, Eric A. Sandvol<sup>1</sup>, James Ni<sup>2</sup>, Tom Hearn<sup>2</sup>, Savas Ceylan<sup>1</sup>, Xiaofeng Liang<sup>1</sup>, and W. Scott Phillips<sup>3</sup>

University of Missouri<sup>1</sup>, New Mexico State University<sup>2</sup>, and Los Alamos National Laboratory<sup>3</sup>

Sponsored by the Air Force Research Laboratory

Award No. FA9453-10-C-0256

Proposal No. BAA10-61

**ABSTRACT**

High-resolution seismic velocity and attenuation models of the Tibetan Plateau and adjacent regions of western China are critical to monitoring seismology efforts in Eurasia. Our waveform data are collected from new deployed seismic networks including NETS (North-Eastern Tibet Seismic experiment), INDEPTH-IV-ASCENT, INDEPTH-IV-UK, and previous networks, comprising an unprecedented coverage of the eastern half of the Tibetan plateau. Three seismic methods are used in the velocity structure in this region:  $P_n$  velocity tomography, body-wave finite-frequency tomography, and Rayleigh wave phase velocity. We observe consistent anomalies in the crust and upper mantle using all of these methods. These anomalies include a low velocity in northern Qiangtang and the Songpan-Ganzi fold belt and the high velocity in the Qaidam Basin.  $Q_{Lg}$  and  $Q_{Pg}$  models have been determined using a Reverse Two-station/event Method, which shows a high seismic attenuation zone along the Kunlun belt. We have also observed significant azimuthal anisotropy of seismic  $Q$ . The isotropic seismic  $Q$ , suggested as an estimate of  $Q_s$  for the crust, is low in northern Qiangtang and the Songpan-Ganzi. The high- $Q$  directions parallel major fault planes in eastern Tibet, and correlate with fast-direction of shear wave splitting and Rayleigh wave azimuthal anisotropy fast directions, which suggests a coherency of deformation between the crust and upper mantle in this region. Similarly, a high velocity and high  $Q$  block in southeastern Tibet around eastern Bangong-Nujiang Suture and Eastern Himalaya Syntaxis correlates well with the high velocity in this region.

## **OBJECTIVES**

The objectives of this project are to establish high-resolution three-dimensional seismic velocity models and regional wave attenuation models for the crust and upper mantle in Tibetan Plateau and adjacent regions of western China. The Tibetan Plateau and adjacent areas have been focused by many studies of seismic velocity structure (e.g., Kind et al., 2002; Tilmann et al., 2003; Li et al., 2008) and seismic attenuation structure (e.g., McNamara et al., 1996; Phillips et al., 2000; Xie, 2002). Reliable high resolution images of the crustal and mantle of this region is very important but limited by insufficient data sets and mutually independent techniques. Our research involves new waveform database, which have increased the coverage of the northern Tibet and Qaidam Basin (Figure 1). All stations are equipped with broadband CMG-3T, CMG-ESP, and STS-2 sensors. Based on the results of last year's research review (Sandvol et al., 2010), we have applied this new data set and various techniques to estimate the seismic velocity and Q variations within this area.

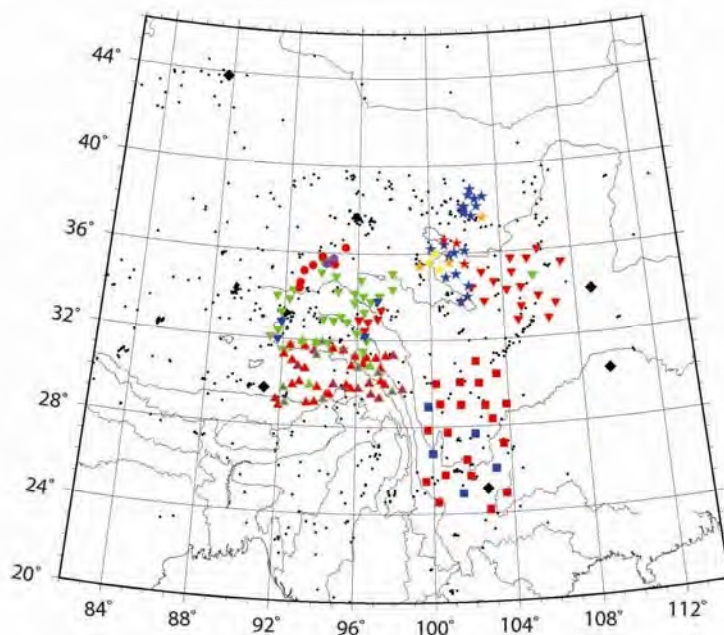


**Figure 1. A map showing the broadband stations from all permanent and temporary networks whose data are used in our project. Inverse triangles represent the experiment ASCENT and stars represent NETS. As other temporary networks deployed across the Tibet, the stations of Namche Barwa, MIT-China, INDEPTH-IV-UK are represented by triangles, squares, and circles, respectively. The black diamonds represent the permanent network CDSN. Different colors are used to illustrate the details of seismometers and dataloggers. The red, green, blue, purple, and yellow symbols represent Streckeisen STS-2, Guralp-CMG3T, Guralp-CMG3ESP, Guralp-CMG40T, and Guralp-CMG3TD (only in NETS experiment) seismometers associated with Reftek-130 dataloggers; the orange symbols (only in NETS experiment) represent Guralp-CMG3TD seismometers associated with Guralp dataloggers; the small purple triangles (only in Namche Barwa experiment) represent stations where Guralp-CMG40T seismometers replaced other seismometer types in deployment.**

## **RESEARCH ACCOMPLISHED**

Using both travel-time body and surface wave tomography, we have created a Pn velocity model, 3-D P and S wave velocity models, and Rayleigh waves phase velocity models for the crust and upper mantle of this region. We have also generated 2-D  $Q_{Lg}$  and  $Q_{Pg}$  models while site and source responses are isolated and resolved as well. A significant azimuthal anisotropy of Q is dramatically observed and solved in 2-D tomography.

### Three Velocity Models

Pn waves mainly travel within a layer closely beneath the Moho discontinuity, and thus its velocity model mainly represents the velocity structure of the uppermost mantle. We have applied the method of Hearn et al. (1991) to generate the Pn velocity tomographic model (Figure 2). The Pn velocity varies from 7.8 km/s to 8.3 km/s with an average of 8.1 km/s. In the Qiangtang and Songpan-Ganzi (Bayan Har) terrane of northeastern Tibet, low Pn velocities are generally observed. A high Pn velocity anomaly is located at the eastern end of the Bangong-Nujiang Suture around the Eastern Himalayan Syntaxis. The Qaidam Basin and Gonghe Basin have high Pn velocities. An abrupt Moho depth change is suggested by the observed significant difference of station delays along Kunlun, the northern margin of the plateau.

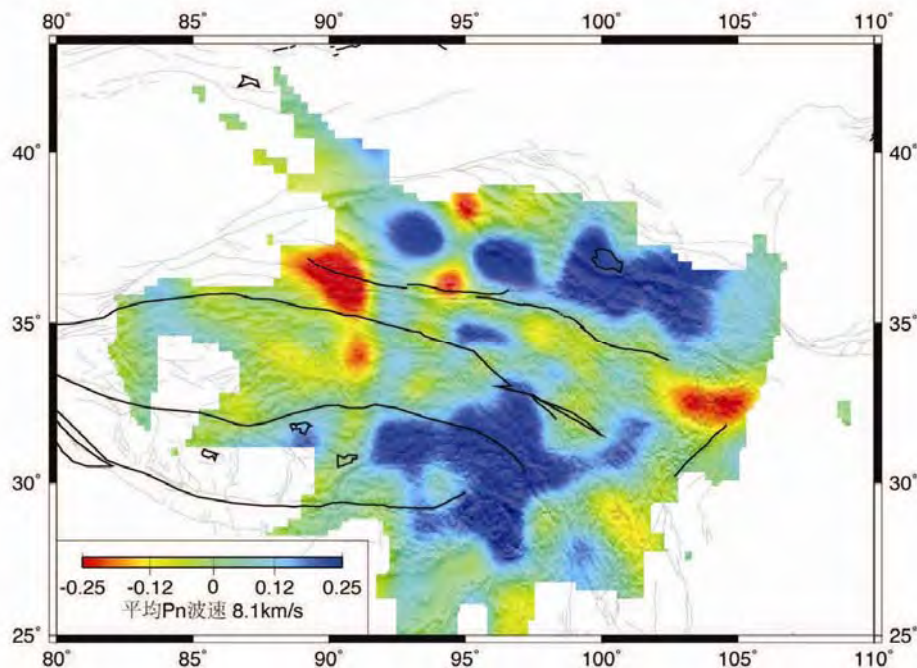


**Figure 2. Pn wave velocity structure in the northeastern Tibetan Plateau. High Pn velocity anomalies are located to the north of the Kunlun range and around the Eastern Himalayan Syntaxis. Low Pn velocity anomalies are mainly observed in central Qiangtang and northern Songpan-Ganzi terrane.**

We have applied a finite-frequency tomography method (e.g., Hung et al., 2004; Liang et al., 2011) to generate three-dimensional P and S body wave velocity models for the lithosphere of the eastern Tibet (Figure 3). A contrast between a widespread slow velocity northern Tibet and heterogeneous southern Tibet is significant in the upper mantle velocity structure. The homogeneous low P- and S- velocity anomalies in the crust and upper mantle of the northern Qiangtang and Songpan-Ganzi terranes probably penetrate into the upper mantle. High P- and S-wave velocity anomalies are generally distributed within the mantle beneath the Qaidam Basin and southern Tibet to a depth of more than 250 km. A few N-S oriented low velocity bands are observed beneath southern Tibet and appear to extend to at least 150 km depth.

A three-dimensional model of fundamental mode Rayleigh waves phase and shear-wave velocities with azimuthal fast directions is also presented for the lithosphere of the eastern Tibet (Figure 4). Like Pn and body wave results, low velocity anomalies occur across and within major strike-slip fault zones in the Qiangtang and Songpan-Ganzi portion of the northern Tibet. A high velocity anomaly is observed along the Bangong-Nujiang Suture at 65 km depth, probably is a portion of the underthrusting Indian plate. Azimuthal fast directions are consistent at all depths up to approximately 200 km, which suggests a vertical coherent deformation in the Tibetan crust and lithospheric mantle. The highest magnitude of azimuthal

anisotropy is observed in northern Tibet with a direction nearly paralleling major fault trend and shear wave splitting fast directions.

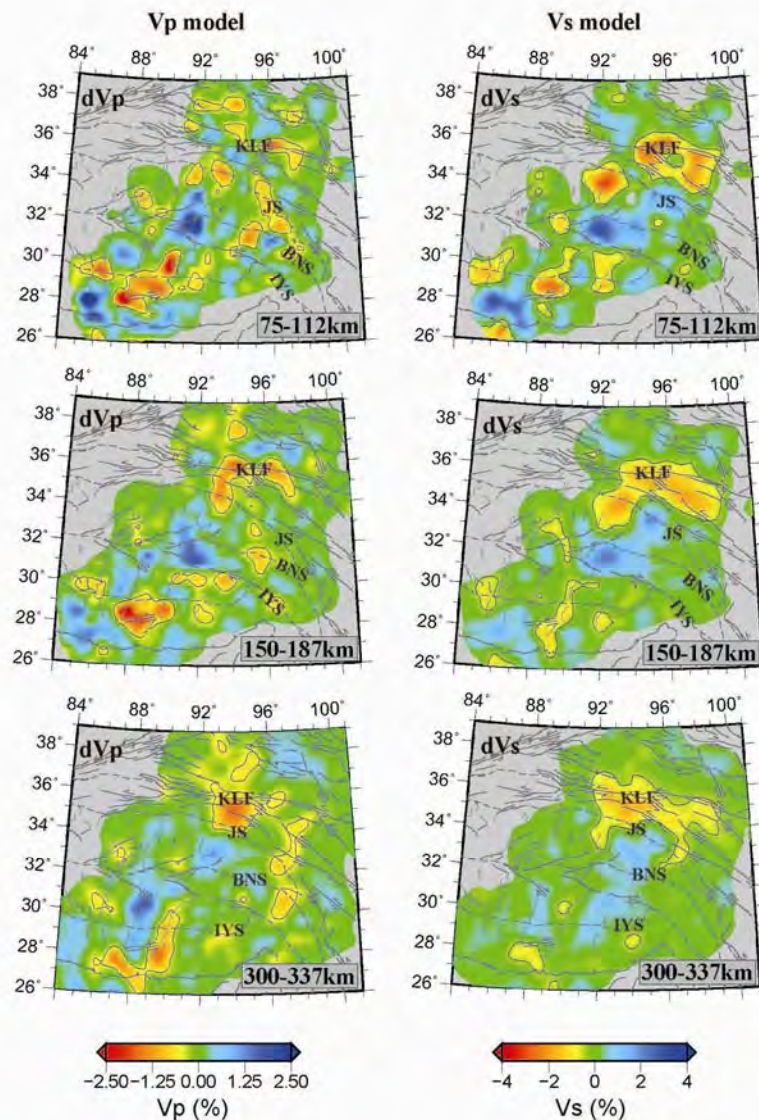


**Figure 3.** Three-dimensional P- and S-wave velocity models for the upper mantle of the eastern Tibet. A significant N-S contrast for both P-wave and S-wave velocity is significant.

All of the methods individual results consistently show a low velocity zone in the northern Qiangtang and Songpan-Ganzi terranes, and relatively high velocity in southern Tibet and Qaidam Basin. The strong correlation between the independent methods suggests that, at least to first order, these models are relatively robust. Further studies are expected to see if these models will help to improve sparse network earthquake locations.

### Seismic Attenuation

$Q_{Lg}$  is typically assumed as an approximation for shear wave  $Q$  of the crust, and is widely used in nuclear discriminants. We used a Reverse Two-station/event Method (RTM) (Chun et al., 1987) to measure accurate path-based  $1/Q_{Lg}$  values. This method is an improvement upon the Two-Station Method (TSM) and includes two specific cases: Reverse Two Station (RTS) path and Reverse Two Event (RTE) path. In theory, it eliminates the contribution on spectral amplitude from the source excitation function, radiation pattern, instrument response, and site response, and has been presented as the most accurate method in  $Q$

measurement (Ford et al., 2008). Because of its rigorous geometrical requirement and the specific propagation characteristics of Lg, the application of this method still requires extensive seismic network deployed contemporaneously throughout Tibet (Fan and Lay, 2003). The deployments of ASCENT and NETS have ideally increased the accuracy and resolution of  $1/Q_{Lg}$  measurements, and furthermore, permit an application of both the RTS and RTE in Tibet.

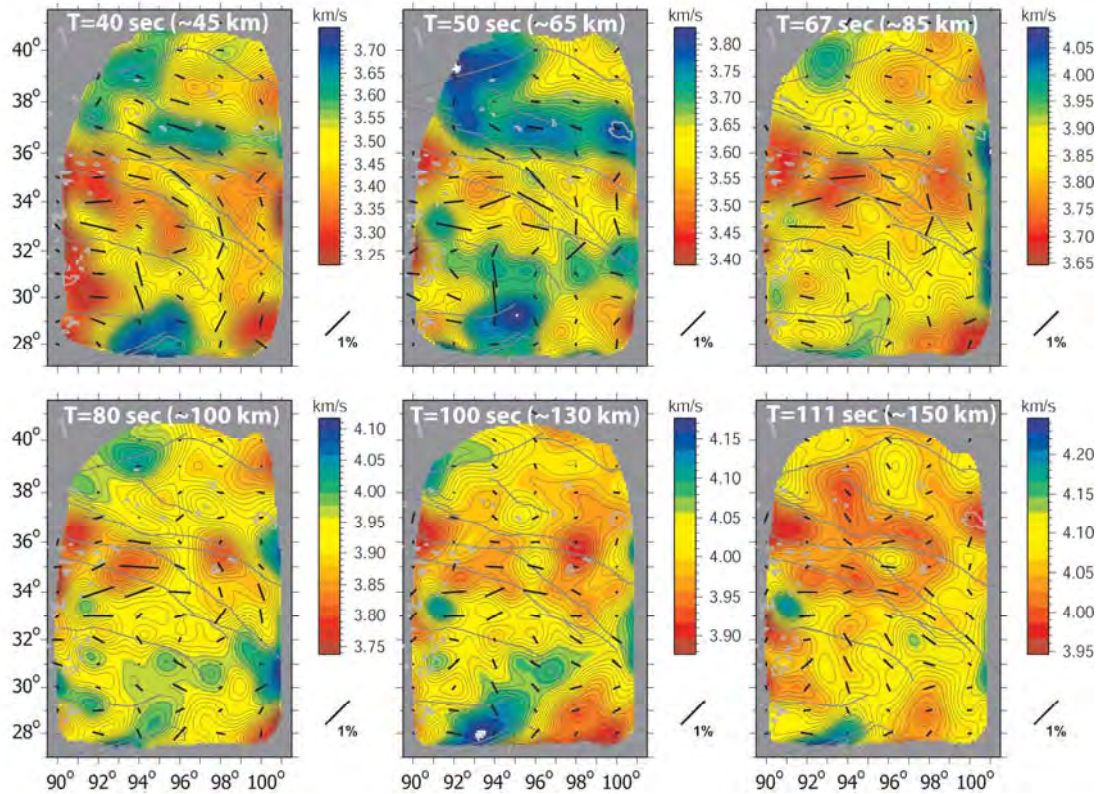


**Figure 4. The 3D model of Rayleigh waves phase velocities with azimuthal anisotropy. Notice the color scale of each section represents different velocity range. Low velocity anomalies and high azimuthal anisotropy magnitude mainly locate within northern Tibet.**

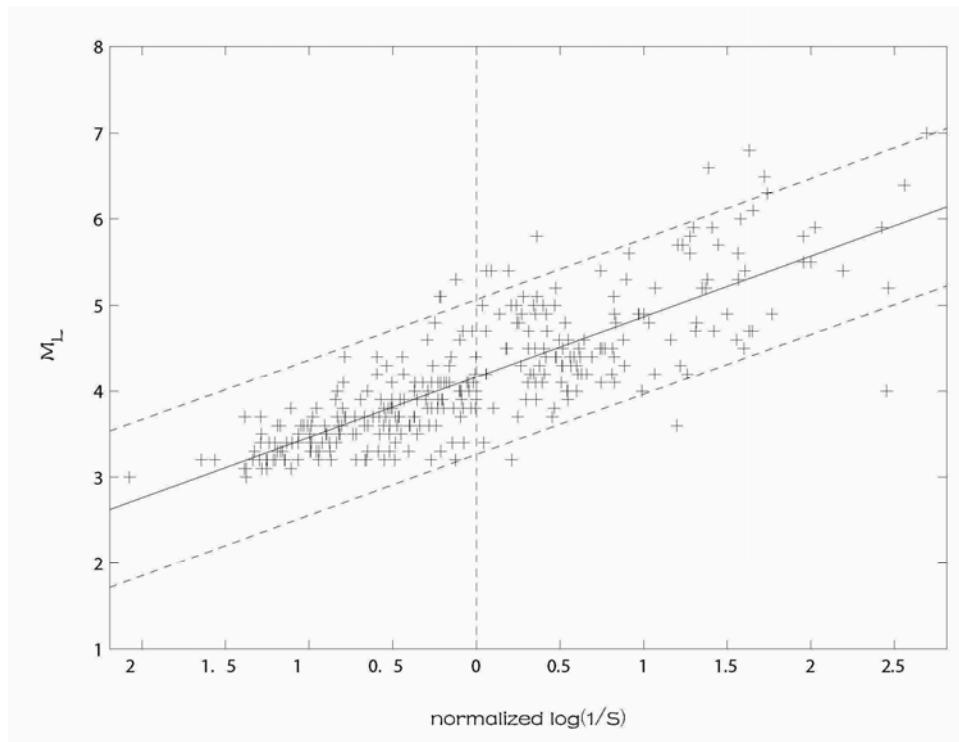


**Figure 5. The nearly linear relationship between logarithm of the reciprocal of normalized RTM Lg source term and magnitude  $M_L$ . The solid line represents the least-square linear fit line and the two dashed lines parallel to it represent its 95% confidence interval.**

We also use the RTM to solve the site response and source response. A significant site response difference is observed between the Tibetan Plateau and major basins, probably dependent on topography or sedimentary thickness. This is very important to studies on moment and ground-motion. Also, a nearly linear relationship is observed between the logarithm of the reciprocal of normalized source term, solved from RTM and Lg spectra, and magnitude  $M_L$  between 3 and 7 (Figure 5). The seismic moment  $M_0$  can be estimated from  $M_L$  (Hanks and Kanamori, 1979). Because the RTM eliminates the contribution of path, site, and radiation pattern, it is applicable in accurately detecting the source magnitude.

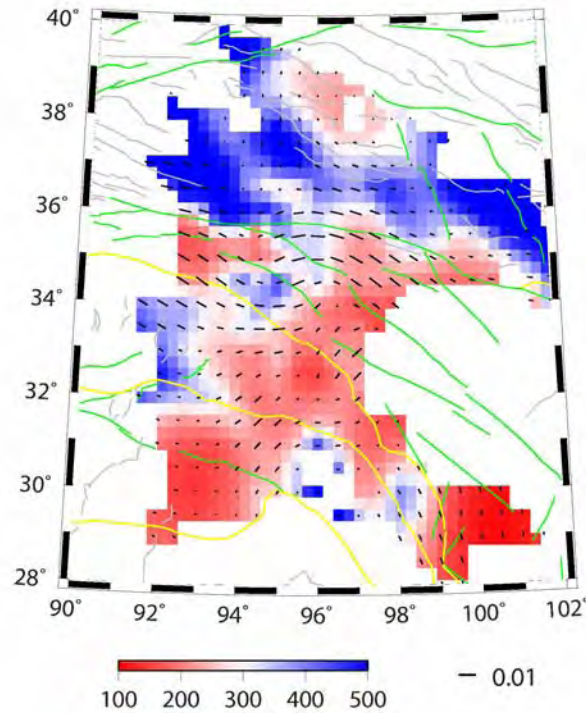


**Figure 6. Imaged variations of isotropic  $Q$ , anisotropy magnitude, and high- $Q$  direction in the crust of eastern Tibetan Plateau at 1 Hz, represented by the color scale and the length and orientation of black vectors, respectively. Major faults and sutures are also shown, while strike-slip faults are green, other types of faults are gray, and sutures are yellow.**

We observe that a strong sinusoidal (or cosinusoidal with a phase shift) relationship between the azimuth and RTM  $1/Q_{Lg}$  values for each inter-station or inter-event paths. Such azimuthal variation in  $1/Q_{Lg}$  has been observed in the western United States (Sutton et al., 1967; Phillips et al., 2009), Tien Shan (Martynov et al., 1999), and southern Tibet (Reese et al., 1999). Similar correlations were derived and widely used for body and surface waves (e.g., Backus, 1965). We have generated a 2-dimensional tomographic model of  $1/Q_{Lg}$  with an azimuthal anisotropy by solving the inverse problem similar with Pn and surface wave azimuthal anisotropy tomography (e.g., Hearn, 1996). Approximately 48,000 four-spectral amplitude groups are collected as input data for the tomography. Resolution tests suggest that an anomaly with the size of  $2^\circ \times 2^\circ$  can be retrieved for the eastern Tibet. Figure 6 shows the model at a frequency of 1 Hz.

The  $1/Q_{Lg}$  azimuthal anisotropy is weakly frequency-dependent within eastern Tibet. There is a strong azimuthal anisotropy of  $1/Q_{Lg}$  within the northern Tibet. The maximum anisotropic magnitude is observed to be higher than 0.01 in the northwestern Songpan-Ganzi terrane, Kunlun range, and northern Qiangtang terrane, while the anisotropic magnitude is very low in the central Qaidam Basin, showing a significant discontinuity along the northern margin of Tibetan Plateau. The high- $Q$  direction is nearly uniformly E-W in the northern Tibet, very similar to the pattern of surface wave azimuthal anisotropy. Furthermore, the high- $Q$  and fast directions parallel major strike-slip fault planes, such as the North Kunlun Fault and South Kunlun Fault. The anisotropic magnitude increases around the Eastern Himalayan Syntaxis, where the high- $Q$  direction likely has a complicated rotation from E-W in the west to NW-SE to the east. By isolating the anisotropy of  $1/Q_{Lg}$ , the isotropic  $1/Q_{Lg}$  is strongly frequency-dependent in the eastern Tibet. The Qaidam Basin has a stable low isotropic  $1/Q_{Lg}$  ( $<1/500$  at 1 Hz) which indicates a cold, stable, and relatively homogenous crust. In northern Tibet, such as the Songpan-Ganzi and Qiangtang terranes, we

observe high isotropic  $1/Q_{Lg}$  ( $1/400 \sim 1/150$  at 1 Hz). A low  $1/Q_{Lg}$  anomaly is also observed near the Eastern Himalayan Syntaxis, which is probably consistent the suggestion of an underthrusting cold Indian crust.

### **CONCLUSIONS AND RECOMMENDATIONS**

In this project, we are processing a large set of new broadband waveform data to obtain three velocity models using Pn, body waves, and surface waves as well as a crustal Q model using a new technique for major portions of western China. The three separate velocity models show consistent results including a low velocity in the northern Qiangtang and the Kunlun belt and a high velocity anomaly within the Qaidam Basin. This suggests a strong lateral variation and vertical coherency of velocity structures for the whole lithosphere in eastern Tibet and adjacent regions. A high seismic attenuation zone is observed along the Kunlun belt where the seismic attenuation has a strong azimuthal anisotropy. The isotropic seismic Q, suggested as an estimate of crustal Q, is low in northern Qiangtang and the Kunlun belt and high in the Qaidam Basin, which corresponds with the crustal velocity models. The consistent patterns of direction distribution of Rayleigh wave azimuthal anisotropy at different depth and Q azimuthal anisotropy suggests a coherency of deformation between the crust and upper mantle in this region.

### **ACKNOWLEDGEMENTS**

We are grateful to all members of the INDEPTH IV and NETS teams, as well the IRIS DMC for providing other seismic data.

### **REFERENCES**

- Backus, G. E. (1965). Possible forms of seismic anisotropy of the uppermost mantle under oceans, *J. Geophys. Res.* 70: 3429-3439.
- Chun, K.-Y., G. F. West, R. J. Kokoski, and C. Samson (1987). A novel technique for measuring  $L_g$  attenuation-results from eastern Canada between 1 to 10 Hz, *Bull. Seismol. Soc. Am.* 77: 398-419.
- Fan, G.W. and T. Lay (2003). Strong  $L_g$  wave attenuation in the Northern and Eastern Tibetan Plateau measured by a two-station/two-event stacking method, *Geophys. Res. Lett.* 30: 1530, doi: 10.1029/2002GL016211.
- Ford, S. R., D. S. Dreger, K. Mayeda, W. R. Walter, L. Malagnini, and W. S. Phillips (2008). Regional attenuation in northern California: a comparison of five 1D Q methods, *Bull. Seismol. Soc. Am.* 98: 2033-2046, doi:10.1785/0120070218.
- Hanks, T. C. and H. Kanamori (1997). A moment magnitude scale, *J. Geophys. Res.* 84: 2348-2350.
- Hearn, T. M. (1996). Anisotropic Pn tomography in the western United States, *J. Geophys. Res.* 101: 8403-8414.
- Hearn, T. M., M. N. Beghoul, and M. Barazangi (1991). Tomography of the western United States from regional arrival times, *J. Geophys. Res.* 89: 1843-1855.
- Hung, S.-H., Y. Shen, and L.-Y., Chiao (2004). Imaging seismic velocity structure beneath the Iceland hot spot: A finite frequency approach, *J. Geophys. Res.* 109: B0835, doi: 10.1029/2003JB002889.
- Kind, R., X. Yuan, J. Saul, D. Nelson, S. V. Sobolev, J. Mechie, W. Zhao, G. Kosarev, J. Ni, U. Achauer, M. Jiang (2002). Seismic images of crust and upper mantle beneath Tibet: Evidence for Eurasian plate subduction, *Science* 298: 1219-1221.
- Li, C., R. D. Van der Hilst, A. S. Meltzer, R. Sun, and E. R. Engdahl (2008). Subduction of the Indian lithosphere beneath the Tibetan Plateau and Burma, *Earth Planet. Sci. Lett.* 274: 157-168.
- Liang, X., Y. Shen, Y. J. Chen, and Y. Ren (2011). Crustal and mantle velocity models of southern Tibet from finite frequency tomography, *J. Geophys. Res.* 116: B02408, doi: 10.1029/2009/2009JB007159.

- Martynov, V. G., F. L. Vernon, R. J. Mellors, and G. L. Pavlis (1999). High-frequency attenuation in the crust and upper mantle of the northern Tien Shan, *Bull. Seismol. Soc. Am.* 89: 215–238.
- McNamara, D.E., T. J. Owens, and W. R. Walter (1996). Propagation characteristics of Lg across the Tibetan Plateau, *Bull. Seismol. Soc. Am.* 86: 457–469.
- Phillips, W. S., H. E. Hartse, S. R. Taylor, and G. E. Randall (2000). 1 Hz Lg Q tomography in central Asia, *Geophys. Res. Lett.* 27: 3425–3428.
- Phillips, W. S., K. M. Mayeda, L. Malagnini, and C. A. Rowe (2009). Developments in regional phase amplitude tomography, *Seism. Res. Lett.* 80:2, 360.
- Reese C., R. Papine, and J. Ni (1999). Lateral variation of Pn and Lg attenuation at the CDSN station LSA, *Bull. Seismol. Soc. Am.* 89: 325–330.
- Sandvol, E. A., X. Bao, J. Ni, T. Hearn, and S. Phillips (2010). High-resolution seismic velocity and attenuation models of western China, in *Proceedings of the 2010 Monitoring Research Review: Ground-Based Nuclear Explosion Monitoring Technologies*, LA-UR-10-05578, Vol. 1, pp. 197–206.
- Sutton, G. H., W. Witronovas, and P. W. Pomeroy (1967). Short-period seismic energy radiation patterns from underground nuclear explosions and small-magnitude earthquakes, *Bull. Seismol. Soc. Am.* 57: 249–267.
- Tilman, F., Ni, J., and INDEPTH III Seismic Team (2003). Seismic imaging of the downwelling Indian lithosphere beneath central Tibet, *Science*, 300: 1424-1427, doi: 10.1126/science.1082777.
- Xie, J. (2002a). Lg Q in the eastern Tibetan Plateau, *Bull. Seismol. Soc. Am.* 92: 871–876.

## DISTRIBUTION LIST

DTIC/OCP

8725 John J. Kingman Rd, Suite 0944

Ft Belvoir, VA 22060-6218

1 cy

AFRL/RVIL

Kirtland AFB, NM 87117-5776

2 cys

Official Record Copy

AFRL/RVBYE/Robert Raistrick

1 cy